Article

Self-Assembly of Surfactants and Polymorphic Transition in Nanotubes

Noriyoshi Arai, Kenji Yasuoka, and X. C. Zeng

J. Am. Chem. Soc., **2008**, 130 (25), 7916-7920 • DOI: 10.1021/ja7108739 • Publication Date (Web): 30 May 2008

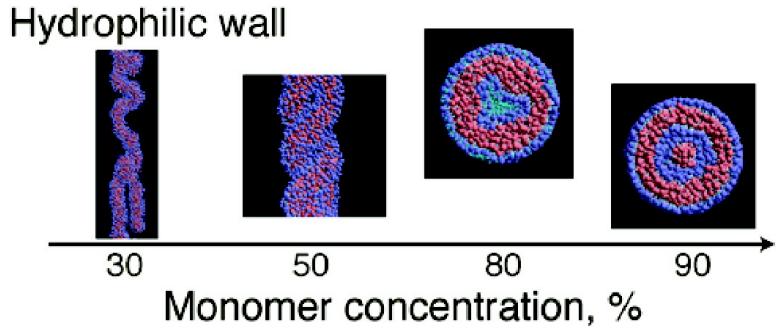

More About This Article

Additional resources and features associated with this article are available within the HTML version:

- Supporting Information
- Links to the 1 articles that cite this article, as of the time of this article download
- Access to high resolution figures
- Links to articles and content related to this article
- Copyright permission to reproduce figures and/or text from this article

View the Full Text HTML

Journal of the American Chemical Society is published by the American Chemical Society. 1155 Sixteenth Street N.W., Washington, DC 20036

J|A|C|S
ARTICLES

Published on Web 05/30/2008

Self-Assembly of Surfactants and Polymorphic Transition in Nanotubes

Noriyoshi Arai,[†] Kenji Yasuoka,*[,†] and X. C. Zeng*[,‡]

Department of Mechanical Engineering, Keio University, Yokohama 223-8522, Japan, and Department of Chemistry, University of Nebraska-Lincoln, Lincoln, Nebraska 68588

Received December 6, 2007; E-mail: yasuoka@mech.keio.ac.jp; xczeng@phase2.unl.edu

Abstract: We study self-assembly and polymorphic transitions of surfactant molecules in water within a nanotube and the effect of water−nanotube interactions on the self-assembly morphologies. We present a simulation evidence of a cornucopia of polymorphic structures of surfactant assemblies—many of which have not been observed in bulk solutions—through adjusting the water−nanotube chemical interactions which range from hydrophilic to hydroneutral and to hydrophobic. The ability to control the morphologies of surfactant assemblies within nanoscale confinement can be used for patterning the interior surface of nanochannels for application in nanofluidics and nanomedical devices.

Introduction

Surfactant molecules such as detergents consist of two chemically distinct functional groups, namely, a hydrophilic head group and a hydrophobic tail group. In bulk solutions, amphiphilic surfactant molecules can spontaneously form a variety of organized assemblies, depending on the concentration of surfactants, the structure of surfactant molecules, and the temperature, among other physical conditions. These organized assemblies include spherical micelles [zero-dimensional (0D) aggregates], cylindrical rodlike and threadlike micelles (1D aggregates), and disklike and bilayer lamellae (2D aggregates).[1–13] This "soft-matter polymorphism" in self-assembly morphologies not only has fundamental relevance in many biological processes but also has been exploited in many industrial and domestic applications. Regardless of the complexity of the assembly structures, it is well-known that the polar head groups of surfactants tend to be exposed to water whereas the nonpolar tail groups tend to be shielded from contacting water by the head groups. The final equilibrium morphology of the surfactant represents a delicate balance between forces involved in chemical interactions among the polar groups, nonpolar groups, and water molecules.

It is also known that fluids confined to nanoscale channels can exhibit distinct phases not shown in the bulk.[14,15] Certain fluids such as water may show abnormal dynamical behavior due to the nanoscale confinement.[16–18] Hummer et al.[16] have revealed a remarkable behavior of transportation of water within a narrow carbon nanotube, in which a chain of hydrogen-bonded water molecules can pass through the tube in a collective fashion. Majumder et al.[17] have shown experimental evidence that fluid flow in carbon nanotubes can be four to five orders of magnitude faster than predicted from conventional fluid-flow theory. Water can also freeze into various polymorphic phases of nanoice in carbon nanotubes.[19–22] At high axial pressure, helical nanoices that resemble helical structures of DNA can also form spontaneously in carbon nanotubes.[23] When the surfactant solution is confined to a nanotube, we expect that much richer self-assembly morphologies can result. Not only the dimensional constraint imposed by the nanotube will affect the thermodynamical equilibrium, but also the added chemical interactions between the nanotube, water, polar groups, and

[†] Keio University.
[‡] University of Nebraska-Lincoln.

(1) Israelachvili, J. N. *Intermolecular and Surface Forces*; Academic Press: London, 1992.
(2) Gelbart, W. M.; Ben-Shaul, A.; Roux, D. *Micelles, Membranes, Microemulsions, and Monolayers*; Springer-Verlag: New York, 1994.
(3) Wendoloski, J. J.; Kimatian, S. J.; Schutt, C. E.; Salemme, F. R. *Science* **1989**, *243*, 636.
(4) Smit, B.; Hilbers, P. A. J.; Esselink, K.; Rupert, L. A. M.; van Os, N. M.; Schlijper, A. G. *Nature* **1990**, *348*, 624.
(5) Zana, R.; Talmon, Y. *Nature* **1993**, *362*, 228.
(6) Karaborni, S.; Esselink, K.; Hilbers, P. A. J.; Smit, B.; Karthauser, J.; van Os, N. M.; Zana, R. *Science* **1994**, *266*, 254.
(7) Danino, D.; Talmon, Y.; Levy, H.; Beinert, G.; Zana, R. *Science* **1995**, *269*, 1420.
(8) Rusling, J. F.; Kumosinski, T. F. *J. Phys. Chem.* **1995**, *99*, 9241.
(9) Manne, S.; Gaub, H. E. *Science* **1995**, *270*, 1480.
(10) Egelhaaf, S. U.; Schurtenberger, P. *Phys. Rev. Lett.* **1999**, *82*, 2804.
(11) Zemb, T.; Dubois, M.; Demé, B.; Gulik-Krzywicki, T. *Science* **1999**, *283*, 816.
(12) Prinsen, P.; Warren, P. B.; Michels, M. A. *J. Phys. Rev. Lett.* **2002**, *89*, 148302.
(13) Jain, S.; Bates, F. S. *Science* **2003**, *300*, 460.
(14) Maddox, M. W.; Gubbins, K. E. *J. Chem. Phys.* **1997**, *107*, 9659.
(15) Mashl, R. J.; Joseph, S.; Aluru, N. R.; Jakobsson, E. *Nano Lett.* **2003**, *3*, 589.
(16) Hummer, G.; Rasaih, J. C.; Noworyta, J. P. *Nature* **2001**, *414*, 188.
(17) Majumder, M.; Chopra, N.; Andrews, R.; Hinds, B. J. *Nature* **2005**, *438*, 44.
(18) Qiao, Y.; Cao, G.; Chen, X. *J. Am. Chem. Soc.* **2007**, *129*, 2355.
(19) Koga, K.; Gao, G.; Tanaka, H.; Zeng, X. C. *Nature* **2001**, *412*, 802.
(20) Maniwa, Y.; Kataura, H.; Abe, M.; Udaka, A.; Suzuki, S.; Achiba, Y.; Kira, H.; Matsuda, K.; Kadowaki, H.; Okabe, Y. *Chem. Phys. Lett.* **2005**, *401*, 534.
(21) Kolesnikov, A. I.; Loong, C.-K.; Zanotti, J.-M.; Thiyagarajan, P.; Moravsky, A. P.; Loutfy, R. O.; Burnham, C. J. *Phys. Rev. Lett.* **2004**, *93*, 035503.
(22) Byl, O.; Liu, J.-C.; Wang, Y.; Yim, W.-L.; Johnson, J. K.; Yates, J. T., Jr. *J. Am. Chem. Soc.* **2006**, *128*, 12090.
(23) Bai, J.; Wang, J.; Zeng, X. C. *Proc. Natl. Acad. Sci. U.S.A.* **2006**, *103*, 19664.

 10.1021/ja7108739 CCC: $40.75

nonpolar groups will definitely disrupt the existing force balance in the free solution. These new chemical interactions can be adjusted to control the molecular organization of surfactants within the nanotube.

Method and Model

We performed dissipative particle dynamics (DPD) simulation[24–27] of a short-chain surfactant/water system confined to a nanotube. The model associated with the DPD method is a coarse-grain model which enables simulation of events occurring within millisecond time scale. The coarse-grain surfactant is a single-chain of soft spheres while the coarse-grain water is just soft spheres. Previous studies have shown that such a coarse-grain model of surfactant/water can reproduce micellar, hexagonal, and lamellar phases with increasing surfactant concentration,[12] the crossing process of threadlike micelles,[26] as well as the self-assembly of long-chain threadlike micelles.[27] A similar coarse-grain model has been used in combination with molecular dynamics to study the self-assembly of diblock copolymers[28] and the adsorption of detergent on a carbon nanotube.[29]

In this study, a surfactant molecule consists of three particles (or monomers): one representing a hydrophilic headgroup (labeled by the letter h) and the other two representing hydrophobic tail group (labeled by the letter t). The nearest-neighbor particles in the surfactant molecule are connected by a harmonic spring with a spring constant of 100 and the equilibrium bond length is 0.86. The water particle (or monomer) is labeled by the letter w. The interactions between any two particles in the solution are described by $a_{ww} = a_{tt} = a_{wh} = 25k_BT$, $a_{ht} = a_{wt} = 70k_BT$, and $a_{hh} = 40k_BT$, where T is the temperature and k_B is Boltzmann's constant. In the DPD simulation, the temperature is controlled as a constant, i.e., $k_BT = 1$.

The inner cylindrical wall of the nanotube is treated as a smooth wall. The potential function of the smooth wall is built based on a structured wall by summing the DPD force between every particle and wall particles.[14] Integration of this summed force results in a force between a particle and the smooth wall (within the cutoff distance r_c), that is, $\mathbf{F}(R)^{wall} = 1/6\pi\rho_{wall}a_{wall,p}(-R^4 + 2R^3 - 2R + 1)\mathbf{R}/R$, where ρ_{wall} is the number density of the structured wall, $a_{wall,p}$ is interaction parameter between the wall and the particle, $\mathbf{R}$ is the normal vector from the wall to the particle, and $R = |\mathbf{R}|$ is the distance between the wall and the particle. Note that the wall-particle interaction is set to be independent of the curvature of the nanotube. The density of the wall particles ρ_{wall} is chosen to be 5.0, the same as the density of surfactant solution.

We have considered three kinds of nanotubes with distinct chemical interactions between water and the nanotube, namely, hydrophobic, hydrophilic, and hydroneutral nanotube. The interaction parameters between hydrophobic wall and water $a_{wall,w}$, and between the wall and the headgroup particle $a_{wall,h}$ are $70k_BT$, and that between the wall and the tail group $a_{wall,t}$ is $25k_BT$. In the case of hydrophilic nanotube, the interaction parameters $a_{wall,w}$ and $a_{wall,h}$ are $25k_BT$ and $a_{wall,t}$ is $70k_BT$. In the case of hydroneutral nanotube, all three interaction parameters are $50k_BT$. The diameter and length of the nanotube are 10.0 and 50.0 in dimensionless units. Details of force formula and interaction parameters have been given elsewhere.[26,27] Here, for the DPD simulation, we used a total number of 19635 particles (monomers). Again, the density of surfactant solution is 5.0 in reduced unit (with the radius of the particles setting at 1).

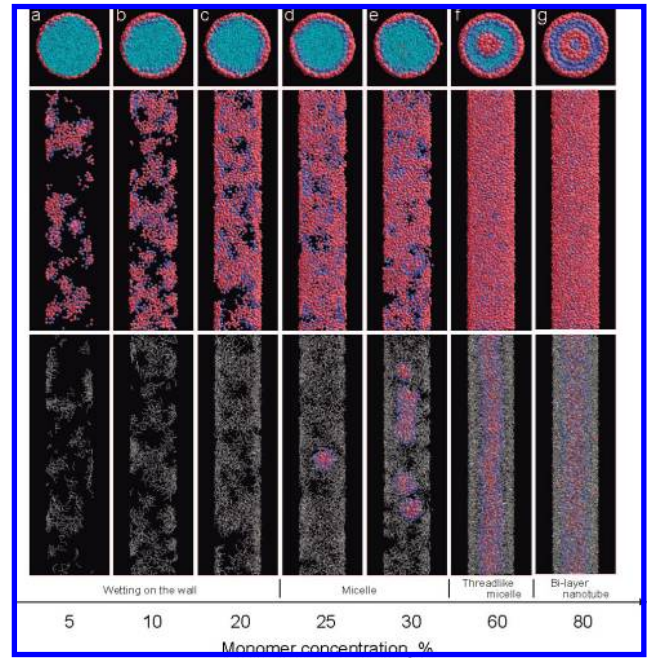

Figure 1. (a−g) Snapshots of equilibrium morphologies of the confined surfactant solution inside the hydrophobic nanotube (not shown in the figure) with increasing the concentration of the surfactant particles (or monomers). The top panel is top views in the axial direction, showing water molecules in blue, the head groups in purple, and the tail groups in pink. The middle and bottom panels are side views of snapshots, where water molecules are removed from the snapshots for clarity. In the bottom panel, the surfactant molecules (in gray) in direct contact with the nanotube are plotted at a much smaller scale to allow a view into the interior surfactant molecules and their morphologies.

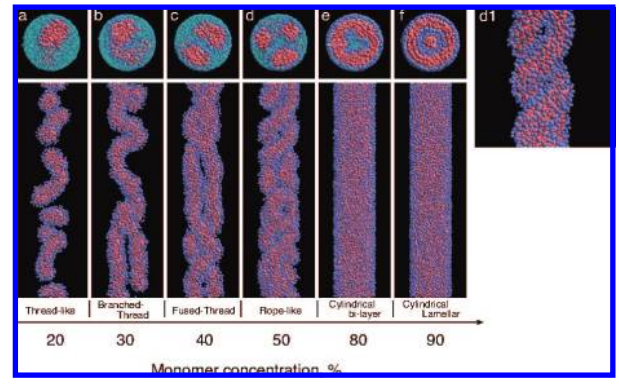

Figure 2. Snapshots of equilibrium morphologies of the confined surfactant solution inside the hydrophilic nanotube (not shown in the figure) with increasing the concentration of the surfactant particles (or monomers). The top panel (a−f) is top views in the axial direction, showing water molecules (blue), the head groups (purple), and the tail groups (pink). The bottom panel is side views of snapshots, where water molecules are removed for clarity. Panel d1 is an enlarged side view of one part of snapshot shown in panel d.

Results

Hydrophobic Wall. In the first series of DPD simulations, we study the surfactant and water confined to a hydrophobic nanotube. In Figure 1, we show snapshots of equilibrium morphologies of the system versus the concentration of the surfactant particles c. The top panel displays top views in the axial direction while the middle and bottom panels display side

(24) Groot, R. D.; Warren, P. B. *J. Chem. Phys.* **1997**, *107*, 4423.
(25) Jury, S.; Bladon, P.; Cates, M.; Krishna, S.; Hagen, M.; Ruddock, J. N.; Warren, P. B. *Phys. Chem. Chem. Phys.* **1999**, *1*, 2051.
(26) Yamamoto, S.; Hyodo, S. *J. Chem. Phys.* **2005**, *122*, 204907.
(27) Arai, N.; Yasuoka, K.; Masubuchi, Y. *J. Chem. Phys.* **2007**, *126*, 244905.
(28) Srinivas, G.; Discher, D. E.; Klein, M. L. *Nat. Mater.* **2004**, *3*, 638.
(29) Wallace, E. J.; Sansom, M. S. P. *Nano Lett.* **2007**, *7*, 1923.

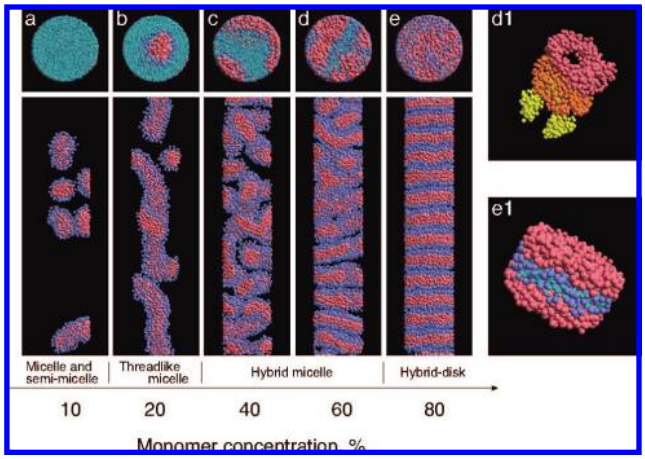

Figure 3. Snapshots of equilibrium morphologies of the confined surfactant solution inside the hydroneutral nanotube (not shown in the figure) with increasing the concentration of the surfactant particles (or monomers). The top panel (a−e) is top views in the axial direction. The bottom panel is side views of snapshots, where water molecules are removed for clarity. (d1 and e1) An elarged side view of one part of snapshot shown in panels d and e, respectively. In panel d1, the head groups and water are removed for clarity; three typical local morphologies of the tail groups are shown in pink, orange, and yellow, respectively, and the orange structure is disklike. In panel e1 water molecules (blue) are included in the enlarged side view.

views of the system with water molecules removed from the picture for clarity. Moreover, in the bottom panel, graphic scales of those surfactant molecules in direct contact with the nanotubes are drastically reduced so that one could look through the nanotube and view morphologies of interior surfactant molecules. As expected, both the top and side views show that the tail groups of the surfactant tend to be in direct contact with the hydrophobic nanotube. At low concentrations, all surfactant molecules are located in the interfacial region between the nanotube and the interior water with their tail groups in contact with the nanotube and their head groups in contact with the water. This contact-layer of the surfactant grows gradually as the concentration (c) increases, until the surfactant completely wets the inner surface of the nanotube at $c \approx 20-25\%$ [Figure 1c bottom panel]. At $c \approx 25\%$, a micelle emerges in the interior region of the nanotube, concomitant with the wetting of the inner surface of the nanotube by surfactant [Figure 1d bottom panel]. At $c \approx 30\%$, multiple micelles can be observed [Figure 1e bottom panel], and 2−3 micelles can fuse into a longer tube-like micelle. At $c \approx 60\%$, a single-strand threadlike micelle occupies the central region of the nanotube. A thin circular water layer is sandwiched between the outer surfactant layer (wetting layer) and the inner threadlike micelle [Figure 1f top panel], where the head groups of both surfactant layers are in direct contact with the water layer. At $c \approx 80\%$, a threadlike inverse micelle forms inside the original threadlike micelle. The combination of the outer and inner threadlike micelles yields cylindrical bilayers [Figure 1g top panel], a structure reminiscent of the bilayer phase that forms in bulk surfactant solution at concentration higher than 80% (see Supporting Information Figure S1).

Hydrophilic Wall. In the second series of simulations, we focus on the surfactant and water confined to a hydrophilic nanotube. In Figure 2, we show snapshots of equilibrium morphologies of the surfactants versus c. In this case, unlike inside the hydrophobic nanotube, the surfactant molecules cannot compete with water molecules to be in direct contact

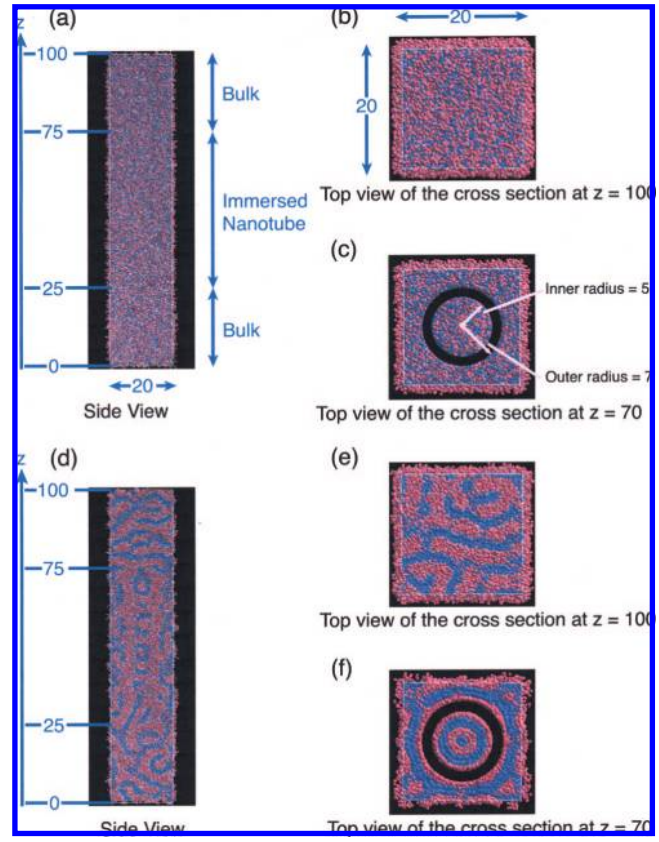

Figure 4. (a) A side view of the system at the initial state. A hydrophobic nanotube (not shown) is immersed in the center of the system (located at $z = 25-75$). The black background is not part of the simulation cell but for the ease of view. Panels b and c are a top view of the cross section of the system at $z = 100$ and $z = 70$, respectively. In panel c, the black ring represents a finite-length nanotube. The thinkness of the nanotube wall is about 2.0. (d) A side view of a snapshot of the system at the equilibrium state; (e and f) top view of a cross section of the system at $z = 100$ and $z = 70$, respectively. Cylindrical bilayers are observed inside the nanotube in panel f.

with the inner surface of the hydrophilic nanotube. In fact, water molecules always wet the inner surface of the hydrophilic nanotube [Figures 2(a−f) top panel] whereas the surfactant molecules tend to stay in the central region of the nanotube with their head groups in contact with water and tail groups shielded from contacting the water. Thus, at very low concentration c, spherical micelles can develop in the central region of the nanotube. At $c \approx 20\%$, multiple threadlike micelles can be observed [Figure 2a bottom panel]. In contrast, in the case of a hydrophobic nanotube and at the same c, even a single spherical micelle cannot be observed. At $c \approx 30\%$, all smaller threadlike micelles merge into a long threadlike micelle that has a branch [Figure 2b bottom panel]. At $c \approx 40\%$, the branch grows into another threadlike micelle and fuses with the original micelle to form a two-stranded thread [Figure 2c]. At $c \approx 50\%$, interestingly, the two-stranded thread evolves into a spiral rope-like micelle where 2−3 threadlike micelles intertwine [Figure 2d]. To our knowledge, a rope-like micelle with a spiral feature [Figure 2d1] has not been observed in bulk solution, suggesting that the rope-like micelle is a new morphology existing only inside the nanotube. At $c \approx 80\%$, the surfactant occupies a major portion of the central region of the nanotube. As expected, the surfactant molecules adopt the cylindrical bilayer morphology [Figure 2e top panel], similar to the case of hydrophobic

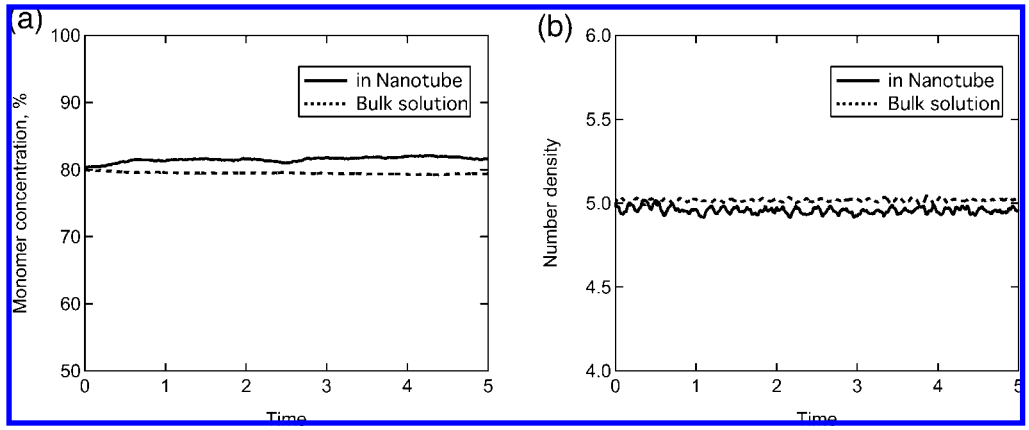

Figure 5. Time versus (a) monomer concentration and (b) number density of the solution inside the nanotube and in the bulk region.

nanotube [Figure 1g top panel]. A closer look at the top panel of Figure 2e finds that a small amount of water is actually trapped in the central region of the cylindrical bilayer micelle. This is because the head groups of the inner surfactant layer can compete with the head groups of the outer surfactant layer to be in direct contact with water. Lastly, at $c \approx 90\%$, the surfactant occupies most of the interior space of the nanotube. To accommodate the closed packing, the surfactant adopts the cylindrical lamellar morphology, analogous to the planar lamellar morphology that typically forms in bulk solution at a very high concentration.

Hydroneutral Wall. In the third series of simulations, we investigate the surfactant and water confined to a hydroneutral nanotube. In Figure 3, we show snapshots of equilibrium morphologies of the surfactants versus c. The hydroneutral nanotube is a unique model in that it neither favors water nor the tail or headgroup of the surfactant molecules. As such, at relatively low concentration $c \approx 10\%$, we observed an intriguing morphology of the coexisting spherical micelles with semimicelles [Figure 3a bottom panel]. In the semimicelles, the head groups of the surfactant are in direct contact with water while the tail groups are shielded from contacting the water through direct contact with the inner surface of the nanotube. The formation of semimicelles can be understood because the tail groups and the water molecules have equal chance to be in close contact with the nanotube, while the head groups always like to be in direct contact with the water. Therefore, the nucleation and growth of the micelle can start either from the central region or on the wall. In the central region, the spherical micelles will develop, whereas on the wall the semimicelles will form. At $c \approx 20\%$, the spherical and semimicelles merge together to form partial threadlike micelles [Figure 3b bottom panel]. Interestingly, the partial threadlike micelles look like "leopard sea cucumber" with nanotentacles in direct contact with the wall. At $c \approx 40\%$, the partial threadlike micelles develop into a highly irregular micelle. The overall framework of the micelle is fractal-like, and so is the pattern of the head or tail groups within the micelle. Thus, this irregular micelle may be described as a hybrid fractal-like micelle. Water is trapped within this fractal-like micelle [Figure 3c top panel] and can no longer percolated through the nanotube in the axial direction. At $c \approx 60\%$, the hybrid fractal-like micelle is cut apart by one or a few disklike micelles as shown in Figure 3d,d1 (orange colored tail groups). Actually, while the outmost part of the micelle (that is in direct contact with the nanotube) shows less patches [Figure 3d bottom panel], most interior parts of the micelle are still highly irregular and fractal-like. Lastly, at $c \approx 80\%$, nearly all the interior space of the nanotube is occupied by the surfactant. Remarkably, the surfactant forms a highly ordered hybrid disklike micelle, which may be also described as a cylindrical lamellar micelle [Figure 3e bottom panel]. Water molecules are pushed out of the central region of the nanotube, and they are only attracted to the headgroups, which [Figure 3e1] form a stack of water rings that surround the lamellar micelle. Again, such a hybrid disklike morphology is unique to the highly confined surfactant in hydroneutral nanotube.

Discussions

The surfactant confined to the hydrophilic nanotube exhibits a sequence of "soft-matter polymorphic" transitions with increasing the surfactant concentration, from the spherical micelle at low concentration, to threadlike micelle and bilayer at medium concentration, and to the lamellar micelle at high concentration. This sequence of transitions is similar to that in the bulk because the hydrophilic nanotube somewhat mimics the water environment surrounding the surfactant so long as the chemical interaction with the surfactant is concerned. Hence, the new morphologies of the surfactant observed inside the hydrophilic nanotube such as the rope-like micelle shown in Figure 2d should be attributed to the effect of confinement. Without the geometric confinement, the rope-like micelle is expected to separate into a number of threadlike micelles as seen in the bulk.[27]

As in the hydrophilic nanotube, the surfactant confined to the hydrophobic nanotube also exhibits a sequence of transitions with increasing the surfactant concentration, namely, from the spherical micelle to the thread-like micelle, and eventually to the bilayer micelle. This similarity in "soft-matter polymorphic" transition can be understood by the following argument: once the inner surface of the hydrophobic nanotube is completely wet by the surfactant monolayer, the hydrophobic nanotube can be viewed essentially as a hydrophilic nanotube (but with a smaller diameter), where the head groups of the wetting monolayer are all pointing inward. Hence, if a hydrophobic nanotube has a diameter about a molecule length-scale larger than a hydrophilic nanotube, one expects that a similar polymorphic-transition sequence would occur for the surfactant confined to both nanotubes.

The surfactant confined to the hydroneutral nanotube shows a dramatically different polymorphic-transition sequence compared to that in the hydrophilic or hydrophobic nanotube. The unique chemical interaction between the hydroneutral wall and

the surfactant (and water) plays a key role in the self-assembly process as well as in the development of the equilibrium morphology, in addition to the effect of geometric confinement. The formation of distinct morphologies such as the semimicelle and hybrid fractal-like micelle is a manifestation of the effect of a unique hydroneutral interaction on the delicate balance among all forces involved in the confined system. Although the hydroneutral nanotube is an idealized model, it does provide a proof of the principle that modification of the chemical characteristics of the inner wall of the nanotube provides an additional degree of freedom to control the self-assembly process and the final equilibrium morphology. Indeed, between the hydrophobic and hydrophilic interaction, there is a large range of chemical interaction one could adjust to modify chemical characteristics of the inner surface. For example, one could molecularly engineer the inner surface of the nanotube with different chemical function groups. Also, one could tailor the chemical pattern of the function groups to control the self-assembly by design.

Further Discussion: A Large-Scale Simulation Test

The simulations presented above were all associated with a closed system, that is, molecule exchanges between the surfactant in the nanotube and the surrounding bulk solution was not considered. In reality, the density and concentration of the surfactant solution within the nanotube can be different from those of the surrounding bulk solution when the nanotube is immersed in a bulk solution. To gain more insights into this difference, we performed a simulation with a much larger system such that molecule exchanges between the surfactant within the nanotube and the surrounding bulk solution is allowed. Specifically, the system involves a finite-length (50) hydrophobic nanotube immersed in a bulk solution (Figure 4). The total number of particles in the system is 181150. The overall density of the surfactant is still 5.0, and the overall concentration of surfactant momomers is 80%. Periodic boundary conditions are applied in all three spatial conditions. The formulation to compute the force between the surfactant and water particles with the nanotube wall is given in the Supporting Information (Figure S2).

We set up two initial surfactant configurations for the simulation, one is uniform as shown in Figure 4, and another is nonuniform, where the nanotube is empty initially (from $z = 25-75$ in Figure 4a). In the latter case, the surfactant solution at other part of the system has a higher density than 5.0. It is found that the final equilibrium state is independent of the initial configuration. In Figure 4d,e, we show a snapshot of equilibrium morphology of the system: Figure 4d is a side view of the system, while Figure 4 panels e and f are a top view of the cross section of the system at $z = 100$ and $z = 70$, respectively. It can be seen from Figure 4f that cylindrical bilayers form spontaneously inside the finite-sized nanotube, as in the case of infinitely long nanotube [Figure 1g top panel]. Moreover, a cylindrical bilayer also forms outside the nanotube, and it is in contact with the outer wall of the nanotube. However, as shown in Figure 4 panels d and e, the transition to the bilayer phase is not seen in the bulk solution because of the presence of nanotubes. As mentioned above, in purely bulk solution, the transition to the bilayer phase occurs at $c \leq 80\%$ (Figure S1). Note that the average concentration of surfactants within the nanotube is about 82% at the equilibrium state (see Figure 5a), which is slightly higher than the overall concentration $c = 80\%$, and the average concentration of surfactants in the bulk is slightly less than 80%. Also, the monomer density (5.02) in the bulk solution is nearly the same as the overall density (see Figure 5b). Hence, a possible reason for the disappearance of the bilayer phase is that the presence of the nanotube shifts the transition point to a higher concentration.

Conclusion

In conclusion, we have performed DPD simulations of self-assembling short-chain surfactant inside different nanotubes. Particular attention is placed on the effect of changing chemical characteristics of the inner wall of nanotube on the surfactant morphologies and polymorphic transitions. Evidence of rich polymorphic structures of the surfactant is revealed for the first time. This study not only enriches the well-known family of polymorphic transitions observed in the bulk solution, but also has practical implication in nanofluidics by chemical modification of the inner surface of nanotube. For example, a hydrophilic nanotube can be produced by anchoring strongly polar molecular groups (e.g., $-$COOH) onto the inner wall of a carbon nanotube. A hydroneutral nanotube can be achieved by anchoring weakly polar molecular groups (e.g., long-chain molecules containing a nonpolar headgroup and a polar group at the middle) onto the inner wall of a carbon nanotube. Extensions of this study to long-chain copolymers,[28,30] long-chain detergent,[29] and peptide amphiphiles[31] are expected to uncover richer morphologies of self-assemblies in different confinement environment.

Acknowledgment. The simulation study was supported by the Core Research for Evolution Science and Technology (CREST) of the Japan Science and Technology Corporation (JST) and in part by the Grant in Aid for the 21st century center of excellence (COE) for System Design: Paradigm Shift from Intelligence to Life from the Ministry of Education, Culture, Sport and Technology in Japan. The theoretical study was supported in part by grants from the NSF (CHEM-0427746, 0701540 and CMMI-0709333), DOE (DE-FG02-04ER46164), and the Nebraska Research Initiative.

Supporting Information Available: Two snapshots of DPD simulation for bulk surfactant solution and the formulation to compute force between surfactant particles and the thin wall of hydrophobic nanotubes. This material is available free of charge via the Internet at http://pubs.acs.org.

JA7108739

(30) Hillmyer, M. A. *Science* **2007**, *317*, 604.
(31) Hartgerink, J. D.; Beniash, E.; Stupp, S. I. *Science* **2001**, *294*, 1684.